







Paleocene-Eocene volcanic segmentation of the Norwegian-Greenland seaway reorganized high-latitude ocean circulation

Jussi Hovikoski ^{1✉}, Michael B. W. Fyhn¹, Henrik Nøhr-Hansen¹, John R. Hopper¹, Steven Andrews ², Milo Barham ³, Lars H. Nielsen¹, Morten Bjerager¹, Jørgen Bojesen-Koefoed ¹, Stefanie Lode¹, Emma Sheldon¹, Alfred Uchman ⁴, Pia R. Skorstengaard⁵ & Peter Alsen ¹

The paleoenvironmental and paleogeographic development of the Norwegian–Greenland seaway remains poorly understood, despite its importance for the oceanographic and climatic conditions of the Paleocene–Eocene greenhouse world. Here we present analyses of the sedimentological and paleontological characteristics of Paleocene–Eocene deposits (between 63 and 47 million years old) in northeast Greenland, and investigate key unconformities and volcanic facies observed through seismic reflection imaging in offshore basins. We identify Paleocene–Eocene uplift that culminated in widespread regression, volcanism, and subaerial exposure during the Ypresian. We reconstruct the paleogeography of the northeast Atlantic–Arctic region and propose that this uplift led to fragmentation of the Norwegian–Greenland seaway during this period. We suggest that the seaway became severely restricted between about 56 and 53 million years ago, effectively isolating the Arctic from the Atlantic ocean during the Paleocene–Eocene thermal maximum and the early Eocene.

¹Geological Survey of Denmark and Greenland (GEUS), Copenhagen, Denmark. ²University of the Highlands and Islands, Inverness, UK. ³Timescales of Mineral Systems Group, School of Earth and Planetary Sciences, Curtin University, Perth, WA 6845, Australia. ⁴Faculty of Geography and Geology, Institute of Geological Sciences, Jagiellonian University, Krakow 3a 30-387, Poland. ⁵Ministry of Foreign Affairs and Energy, Government of Greenland (Nuuk), DK-3900 Nuuk, Greenland. ✉email: jhov@geus.dk

Seaways and marine gateways connecting high- and low-latitude oceans typically influence global climatic systems by affecting salinity and water temperature, and therefore ocean circulation. During the Paleocene–early Eocene (Danian–Lutetian), the Arctic region was affected by continental breakup and seafloor spreading in the Labrador Sea/Baffin Bay, North Atlantic and Eur-

asian basins, and associated North Atlantic igneous province (NAIP) volcanism (Fig. 1a; e.g., see refs. ^{1,2}). The plate movements caused compressional uplift over parts of the Arctic region (Gakkel and Lomonosov Ridges, North Greenland, and Svalbard) and coeval formation of deep subsiding basins (e.g., SW Barents Sea and Eurasian Basin)^{3–10}. Although it is evident that these tectonic processes

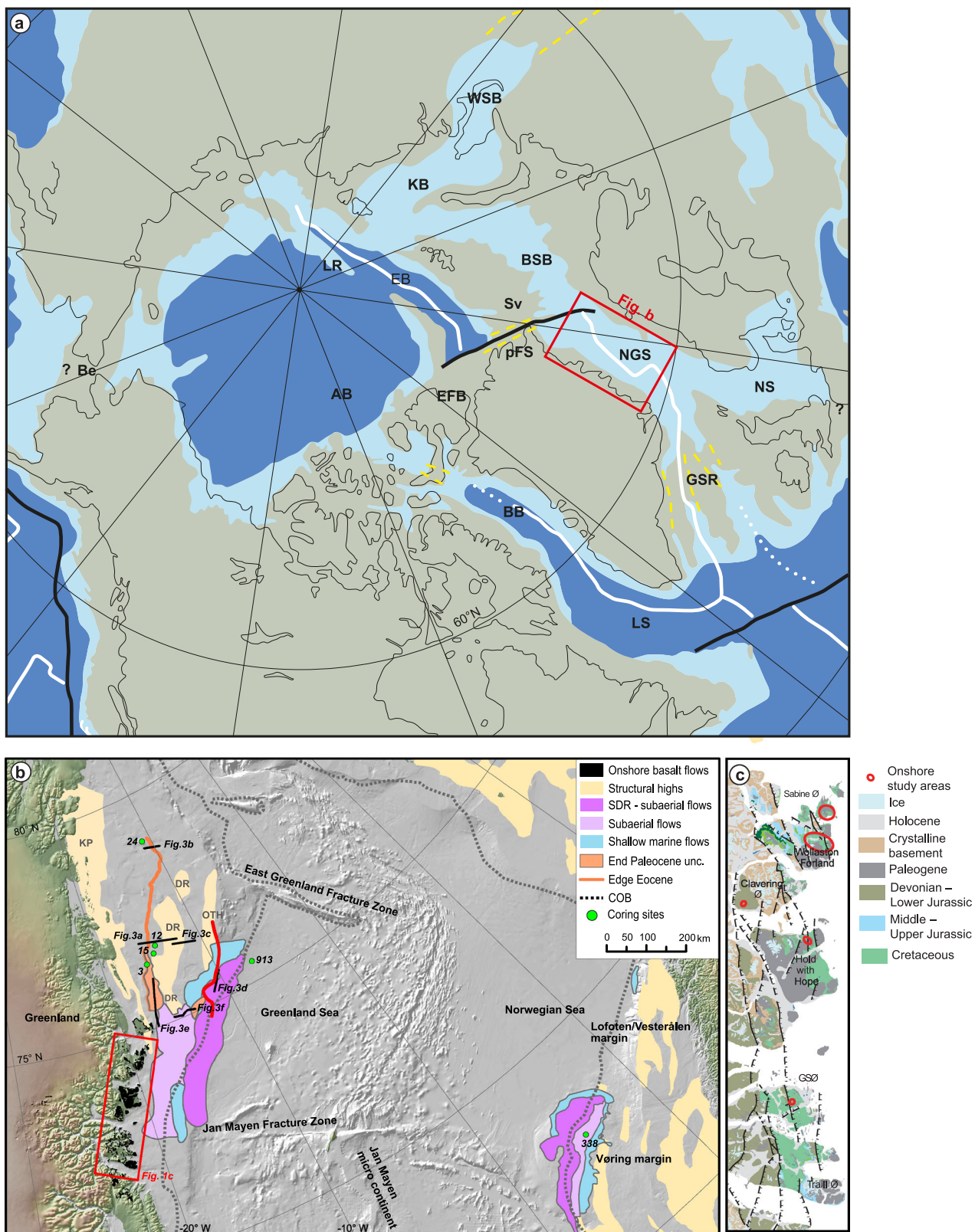


Fig. 1 Paleogeographic setting and study area. **a** Paleogeographic model of the Boreal–Arctic region during the Ypresian (~50 Ma), showing the main geological elements discussed in the text (modified from Blakey¹⁵). AB, Amerasian Basin; BB, Baffin Bay; Be, Beringia; BSB, Barents Sea Basin; EB, Eurasian Basin; EFB, Eureka Fold Belt; GSR, Greenland–Scotland Ridge; KSB, Kara Sea Basin; LR, Lomonosov Ridge; LS, Labrador Sea; NGS, Norwegian–Greenland Seaway; pFS, pre-Fram Strait; Sv, Svalbard; WSB, Western Siberian Basin. Yellow dashed line, transient sea connection; white and black lines, plate boundaries (extensional and transform, respectively). **b** Regional map of the Norwegian and Greenland seas, and surrounding margins. Simplified volcanic elements map includes the main seaward dipping reflector (SDR) sequence related to the main Atlantic opening, additional subaerially erupted basalt flows, and volcanic units interpreted as flows erupted in shallow water. Volcanic elements off Greenland are new interpretations here and elements off Norway are based on Berndt et al.⁷⁹. A major Paleocene unconformity mapped in the seismic data is highlighted by the orange polygons and the light orange line is the landward edge of the Eocene units. The continent–ocean boundary is from Hopper et al.⁸⁰. Red box shows extent of detailed onshore map presented in Fig. 1c. Black lines are seismic profiles in Fig. 3 as labeled. The thick red line indicates the location of potential contourites (Fig. 3d). Numbered green dots are DSDP and ODP sites (338 and 913, respectively), and Kanumas shallow coring project sites. East Greenland margin offshore structural features are: KP, Koldewey Platform; DR, Danmarkshavn Ridge; OTH, Outer Thetis High. **c** Simplified geological map of Northeast Greenland⁸¹ illustrating the main onshore study areas. GSØ, Geographical Society Ø.

must have had profound impacts on high-latitude ocean circulation, the area's paleographic evolution and Paleocene–Eocene water body connectivity remain poorly known in many respects.

During the Paleocene–early Eocene, the Arctic region was variably connected to lower-latitude oceans, in particular through two long, meridional seaways: the Turgay strait (or Western Siberian seaway) and the Norwegian–Greenland seaway (NGS; the focus of this study; Fig. 1a)^{11–15}. Several studies have suggested that the meridional seaways played an important role in the development and decline of the early Paleogene greenhouse climate, including the Paleocene–Eocene thermal maximum (PETM, roughly 56 Ma^{16,17}). Paleogeographic modeling has indicated that even relatively minor changes in seaway morphology and connectivity between the Arctic and Atlantic Oceans could have had profound effects on ocean circulation^{18–22}. In addition, it has been proposed that a restriction of the NGS could have contributed to increasing salinity and sea surface to mid-depth water temperatures in the North Atlantic, and destabilization of marine methane hydrates^{18,19}, in turn contributing to the rapid rise in global temperature during the PETM. Moreover, restrictions of the boreal seaways may have contributed to methane generation²³ and freshening of the Arctic Ocean during the Eocene^{11,19}.

The NGS was initiated during the Jurassic as an intracratonic seaway separating Greenland from Norway²⁴. This incipient NGS persisted into the early Eocene, during which time lithospheric breakup commenced between the East Greenland Fracture Zone in the north and the southern tip of Greenland (around chron C24n.3n 54–53.4 Ma)^{25,26}. The breakup was accompanied by voluminous magmatism associated with the underlying Icelandic hotspot south of the study area^{27,28}. Subsequent changes in spreading kinematics and plate motions shaped the present configuration of the NGS, resulting in a mid-Eocene–Miocene breakup between the East Greenland Fracture Zone and the Arctic Ocean, and the dislocation of the Jan Mayen Microcontinent from Greenland south of the Jan Mayen Fracture Zone^{25,26}.

Despite the potential significance of the NGS for understanding of Paleogene climatic dynamics, its paleoenvironmental and paleogeographic development during the Paleocene–early Eocene has remained inadequately documented. Previous research has focused on the Greenland–Scotland ridge (GSR)—a poorly understood morphological feature generated by uplift and volcanism that has strongly influenced the deep water exchange between the North Atlantic and NGS since the Paleocene^{29–33}. In contrast, the main body of the more than 1500 km-long NGS has received much less attention. Although Paleogene strata have been studied in outcrop along the north-east (NE) Greenland margin^{34,35}, in offshore wells^{36–38}, in seismic sections, and seafloor samples^{39–43}, a coherent

account of the Paleocene–early Eocene development of the NGS and its wider paleogeographical implications is still lacking. This study aims to reduce this knowledge gap by reconstructing the Danian–Lutetian (here restricted to ~63 to ~53 and ~48 to ~47 Ma) paleoenvironments of NE Greenland using integrated sedimentology and palynology. The onshore data are combined with available offshore core data and interpretation of a large grid of generally high-quality two-dimensional (2D) seismic reflection data that document the offshore distribution of the Ypresian subaerial lavas and a coeval subaerially formed unconformity (Fig. 1; see Methods). The study benefits from newly discovered outcrops (Wollaston Forland, NE Greenland) and four shallow boreholes (Kanumas sites 3, 12, 15, and 24), which provide seismic age ties and improve onshore-to-offshore correlations. The data allow investigation of the timing, speed, and magnitude of any restriction and re-opening of the northern part of the seaway during the Danian–Lutetian. Our data, combined with previous research, indicate that the seaway was fragmented into isolated marine water bodies during the Ypresian. The Greenland–Norway Ridge (GNR), as documented and named here, contributed to disruption or major restriction of meridional current activity, in particular between ~56 and ~53 Ma. The first indications for bottom current activity appear in the Lutetian section. The revised basin physiography provides important constraints for paleogeographic and climatic models for the PETM and the early Eocene, which are regarded as an analog for a future greenhouse world.

Results and interpretation

We examined sedimentological, palynological, and seismic characteristics of Danian–Lutetian deposits in outcrops, on a large grid of reflection seismic profiles and in selected wells in the ~700 km-long stretch from Geographical Society Ø (GSØ) in the south to the Danmarkshavn Basin in the north (Figs. 1 and 2). The paleoenvironmental evolution is summarized below. Additional information regarding facies associations, key fossils used in biostratigraphic dating, seismic sections, and paleoenvironmental development are presented in supplementary items (Supplementary Notes 1–4, Supplementary Tables 1 and 2, and Supplementary Figs. 1–15).

Danian–Thanetian (~63–56 Ma). The onshore and core data show that the oldest Paleogene deposits (Danian–Selandian) rest unconformably on Cretaceous sediments (Fig. 2). The sediments are dominated by coarse-grained gravity flow units that intercalate with marine mudstones of offshore and prodeltaic affinities (Supplementary Notes 1, Supplementary Tables 1 and 2, Supplementary Figs. 1–3). At least two major hiatus formed through episodes of fault block rotation and uplift (Fig. 2) during the interval. The latter interpretation is supported by abundant

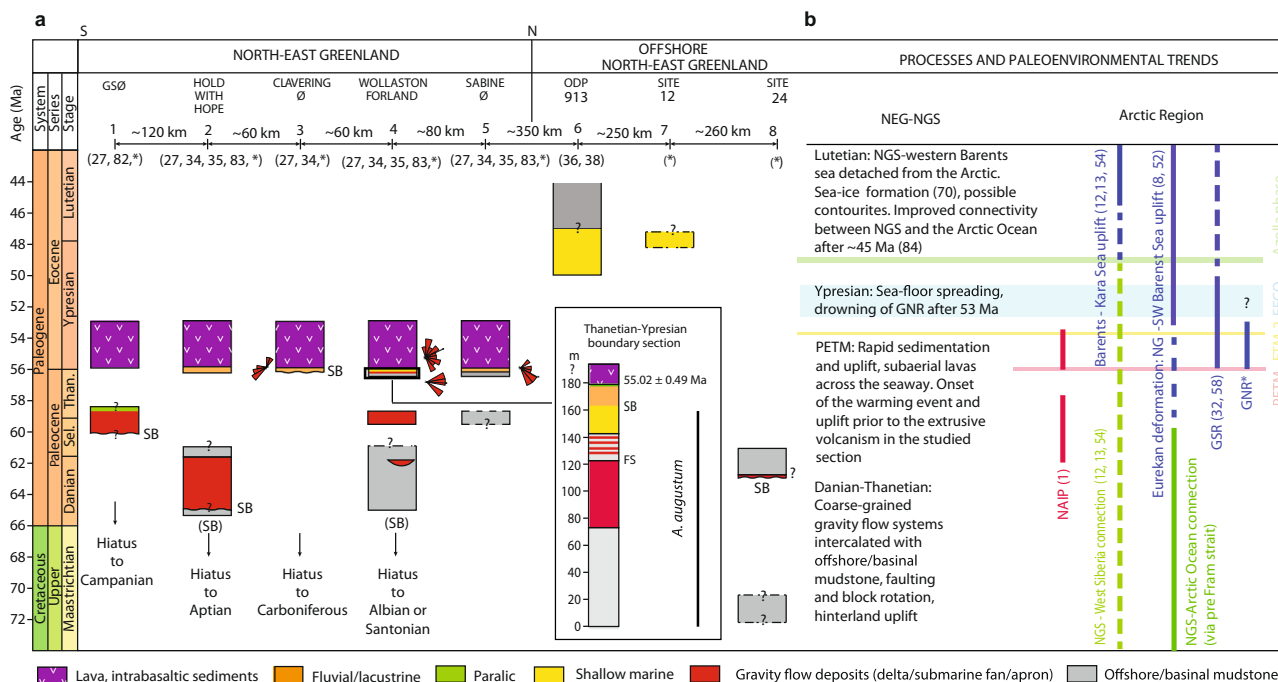


Fig. 2 Stratigraphy and paleoenvironmental trends. References used^{1,8,12,13,27,32,34–36,38,52,54,58,70,82–84} are shown in parentheses. A star refers to locations described in this study. **a** Stratigraphic correlation panel of NE Greenland and offshore coring sites. See Fig. 1 for locations. Radiometric age of lava shown in the inset is from Larsen et al.²⁷ and represents the oldest lava in a nearby locality. GSØ, Geographical Society Ø; SB, Sequence boundary; (SB), inferred, Sel-Selandian, Than-Thanetian. **b** A summary of the main paleoenvironmental trends in NE Greenland (NEG) and estimated occurrence of main tectonic and magmatic events affecting connectivity of the Norwegian–Greenland Seaway (NGS) to other Arctic areas. EECO, early Eocene climate optimum; ETM2, Eocene Thermal Maximum 2; GNR, Greenland–Norway Ridge; GSR, Greenland–Scotland Ridge; NAIP, North Atlantic Igneous Province (main activity); NGS, Norwegian–Greenland seaway; PETM, Paleocene–Eocene Thermal Maximum.

reworked Cretaceous dinocysts, suggesting that marine Cretaceous deposits were exposed and subject to erosion in the catchment area (Supplementary Notes 2). Finally, most of the Thanetian is missing onshore NE Greenland, indicating another possible hiatus.

The Danian to Thanetian interval offshore in the southern Danmarkshavn Basin comprises gently inclined, eastwards prograding clinoforms that cover the Danmarkshavn Ridge following the Cretaceous uplift (Fig. 3a). Farther north along the continent–ocean boundary (COB), footwall uplift associated with a pulse of rifting resulted in the formation of an unconformity and the absence of lower Paleocene strata on structural highs (Fig. 3b). On the outer margin to the southeast, the Danian–Thanetian succession intercalates with the oldest Paleocene lavas in the area (possibly as old as 62–61 Ma similar to the oldest basalts in the northeastern Atlantic²⁷). The basalts have “rubbly” top reflections and a hummocky to internally chaotic reflection pattern suggestive of subaqueous eruption (Fig. 3d, f).

Latest Thanetian–early Ypresian (~56–53 Ma). The interval corresponding to the PETM (latest Thanetian–earliest Ypresian; Paleocene–Eocene boundary; roughly ~56 Ma) is well-developed onshore in the Wollaston Forland area reaching a thickness of almost 200 m (Fig. 2 and Supplementary Notes 1, 2, and 4). The age of the interval is constrained by the distribution of short-ranging dinocysts *Axioidinium augustum*¹⁶ supplemented with previously published radiometric dating of the overlying lower lava series from the area (55.02 ± 0.49, 55.42 ± 0.92, and 55.52 ± 0.68 Ma)²⁷. The lower part of the succession contains a ~60 m-thick gravity flow system typified by deposits of sustained high-density turbidity currents, which are overlain by shallow marine and paralic deposits such as a delta or embayment margin

(see insert in Fig. 2, Supplementary Notes 1 and 4, and Supplementary Figs. 2–4).

The paralic deposits are erosionally overlain by coarse-grained, cobble-bearing fluvial channels, which are locally interbedded with coastal plain and floodplain sediments such as coal layers (Supplementary Figs. 5 and 6). The rapid progradation and the basal erosional contact are interpreted to reflect a forced regressive event (sequence boundary). In a single locality, the erosional contact carves into Carboniferous rocks (Fig. 2; see also ref. 34). Collectively, these facies and stratigraphic relationships indicate an uplift pulse associated with block faulting during the PETM immediately before the initiation of flood basalt magmatism.

In offshore areas, the intra-PETM sequence boundary can be traced to the southern Danmarkshavn Basin and also exists near the COB (Fig. 3e). In the Danmarkshavn Basin, the unconformity formed through subaerial uplift after intrusion and magmatic inflation of the subsurface. The surface, and the interval located up to a few tens of meters above it, is marked by kilometer-wide hydrothermal vent craters connected to the underlying intrusions (Fig. 3e). The vents are interpreted to correspond to a pulse of intense magmatism⁴⁴. A similar stratigraphic surface speckled by volcanic vent craters exists offshore Central Norway and the western UK. Most volcanic vents of the area terminate in this surface dated as 55.8–55 Ma and correlated with the early part of the PETM^{45,46}.

Flood basalt emplacement that started during the PETM lasted until ~53 Ma onshore NE Greenland²⁷. Our data show that scattered intra-basaltic fluvial sediments and weathered top surfaces of lava beds are widespread and indicate common subaerial environments (Supplementary Fig. 6). Moreover, basalt clast-bearing mass flow units more than 20 m thick are also

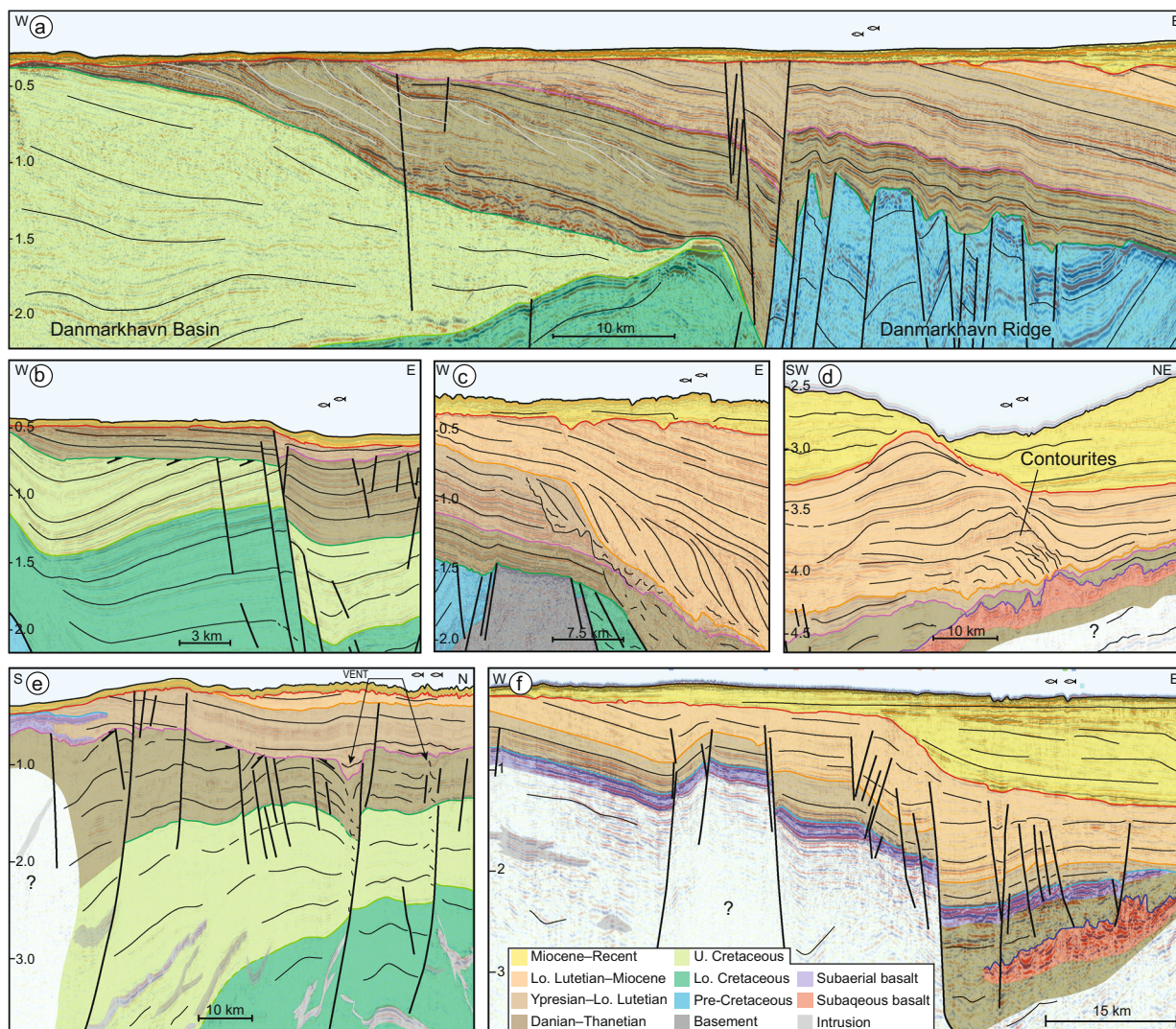


Fig. 3 Offshore seismic examples in two-way travel time. **a** Maastrichtian–Paleocene clinoforms prograding across the Danmarkshavn Basin and burying the Danmarkshavn Ridge for the first time since the Jurassic. **b** Top-Cretaceous unconformity related with down-faulting, footwall uplift and rotation (TGS line NEG15-21880). **c** Earliest Cenozoic burial of the Danmarkshavn Ridge, which consists of Paleozoic strata and basement (TGS line NEG12-2050). **d** Interpreted Paleocene subaqueous basalt, and further up section, mid-Eocene to recent contourite deposits (ION-GXT line NEG1-5500). See Fig. 1b for location. **e** Near-top Thanetian unconformity associated with magmatic intrusions, hydrothermal vents, and the onset of subaerial flood basalt volcanism (TGS line NEG08-101B). **f** Danian–Thanetian subaqueous basalt and lower Ypresian subaerial flood basalts and Paleocene–Eocene down-faulting (TGS line NEG12-2040). The color code applies throughout. Correlations between **a**, **c**, and **d**, and core wells treated in the text are presented in Supplementary Notes 3.

locally present and suggest that relief and instability developed during the continental breakup. The basalts extend offshore south of $\sim 75^{\circ}30'N$ showing a smooth top seismic reflection and generally conformable internal reflections typical for subaerially extruded lavas (Fig. 3f). The offshore flood basalts rest on the near-base Paleocene unconformity. They grade eastwards into seaward dipping reflectors located up to ~ 20 km inboard of the oldest identified magnetic ocean spreading anomaly (chron C24n.3n 54–53.4 Ma²⁵), indicating volcanism and widespread subaerial conditions immediately prior to, and during, initial NE Atlantic opening.

Late Ypresian–earliest Lutetian (~ 53 to ~ 47 Ma?). Post-basaltic Paleogene sediments (<53 Ma) are not observed onshore NE Greenland. Offshore, upper Ypresian deposits (~ 50 Ma) have been reported from Ocean Drilling Program (ODP) site 913 (Fig. 1)^{36,38}. Here, the late Ypresian interval (49.3–48.3 Ma) contains a mix of marine dinocysts and *Azolla massulac*^{11,47} and is interpreted to have

formed in a shallow-water environment³⁶. This is consistent with a contemporary subaerial angular unconformity over structural highs located at the outermost margin and an absence of lower Eocene sediments over the more elevated parts of the early Eocene ocean crust (C24–C22n). Farther inboard, in the southern Thetis Basin, the interval grades into a succession deposited in a few hundred meters of water and fringed to the west and southwest by a steep shelf slope (also described by Petersen³⁹) (Fig. 3c). The shelf slope prograded northeastwards over the Thetis Basin starting in the Ypresian and continuing into the Lutetian. The position of the delta and the direction of sediment transport were most likely controlled by the presence of the basalt traps to the south and southeast, acting as a topographic barrier deflecting the fluvial transport towards the north–northeast (Fig. 4). This is similar to the volcanically deflected Paleocene–Eocene deltaic deposits on the West Greenland margin^{48,49}.

The offshore Kanumas coring site 12 in the Danmarkshavn Basin intersected the uppermost Ypresian and lowermost Lutetian (~ 47.8 Ma) located inboard of the shelf break (Fig. 1

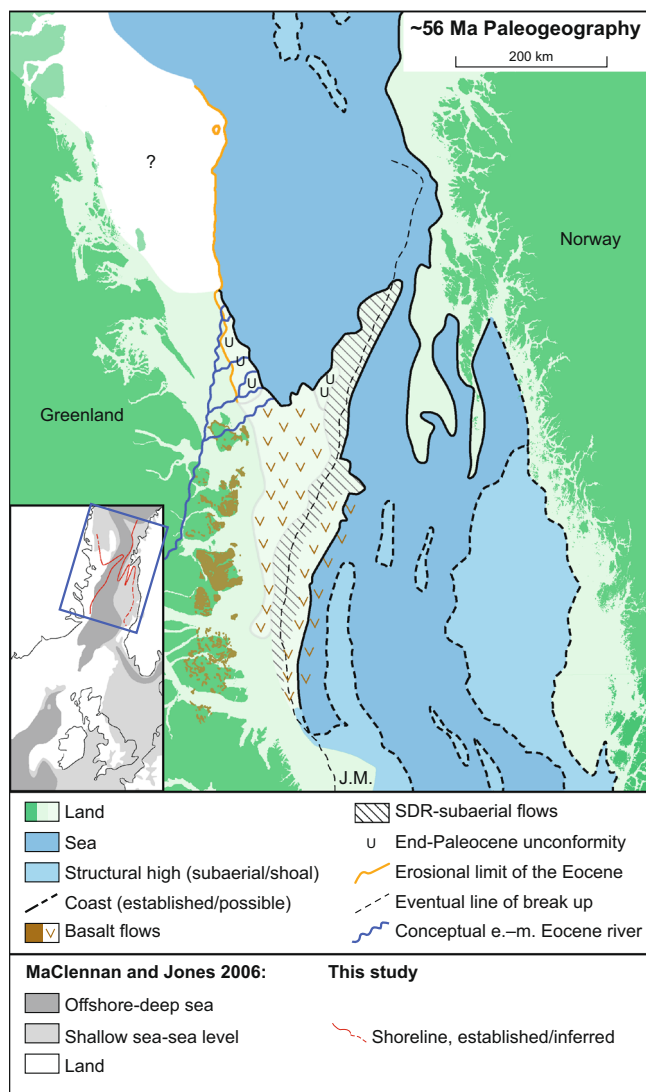


Fig. 4 Greenland-Norway Ridge during the Paleocene-Eocene transition.

G-Plate reconstruction based on the poles of rotation and compilation of magnetic anomalies of Gaina et al.²⁵ with mapped volcanic facies and subaerial unconformities projected onto establish the distribution of land and sea. See the “Methods” section for detailed approach. The inset figure shows the paleogeography of the greater NGS region, which is modified and simplified from the uplift model of Maclennan and Jones³⁰ for the same time period. The data presented here revise the paleogeography of the main body of NGS. Instead of deep sea continuation towards the Barents Sea, the northern NGS was almost closed by a volcanic ridge at least until ~53 Ma. A narrow shallow-water strait may have existed between Greenland and Europe.

and Supplementary Note 2). The cored succession formed in a storm- and wave-influenced shallow marine environment (Fig. 2, Supplementary Notes 1, and Supplementary Fig. 7). The upper Ypresian to lowermost Lutetian succession covers the subaerial basalt flows located offshore south of N 75°.

Above the upper Ypresian to lowermost Lutetian marginal marine section in the ODP site 913, an early Lutetian (~47 Ma) transgression denotes the onset of deep-marine deposition^{36,38}. Away from the borehole, this transgressive interval roughly corresponds to the oldest contourite moats and drifts along the COB interpreted based on their geometry in seismic data, suggesting the onset of deep-marine conditions over the oldest ocean crust (Fig. 3d and Supplementary Fig. 15). These

contourites make up the lowermost part of a kilometer-thick succession of contourites that extends all the way to the Recent and influences the relief of the modern shelf slope. Although distinct in outline, these Eocene drift and moats are smaller in scale compared with the younger contourites. Future work should include further drilling to improve the stratigraphic control of the succession.

Discussion

Previous paleoclimatic and paleoceanographic modeling has indicated that the paleogeography of the NGS, and its connection to the Arctic region, may have had a major impact on Atlantic meridional overturning circulation and North Atlantic bottom water temperature during the Paleocene–Eocene^{18–22}. Two possible sea connections linked the NGS to the Arctic Ocean during this time: the pre-Fram strait area between North Greenland and Svalbard, and Barents shelf–Kara Sea areas (Fig. 1a¹⁵). Various paleogeographic models exist for the Paleocene–Eocene Arctic area^{13,14,50,51} due to a lack of preserved sedimentary record (eastern Barents Sea, Kara Sea) and uncertainties pertaining to the timing of tectonic events. Key tectonic events include seafloor spreading in the North Atlantic (~54 Ma onwards)²⁶, which led to northward movement of the Greenland plate, and compression and uplift in the pre-Fram strait area, eventually terminating the shallow marine connection between Svalbard and Greenland (Fig. 2). Recent apatite fission track data from North Greenland suggest that the area may have experienced onset of uplift around the Selandian (~60 Ma)⁵², whereas the first main Eureka compressional phase may have taken place during the Ypresian–Lutetian (53–47 Ma)⁸. The translational tectonics associated with the Eureka orogeny also affected the SW Barents Sea area and led to the development of deep transtensional basins, as well as basement ridges that restricted marine connections towards the east^{9,10,50}. However, similarities in dinocyst assemblages between western Siberia and the North Sea Basin suggest that temporary shallow marine connections existed across the Barents Sea at least until the early Lutetian, when a major regression detached the Western Siberian seaway from the Arctic Ocean^{12,53–55}.

Basin morphology and the timing and degree of opening and restriction of the NGS during this time have remained poorly understood. Challenges include the NAIP emplacement-related punctuated uplift and a consequent incomplete stratigraphic record (e.g., along GSR and in NE Greenland), limited biostratigraphic constraints, or lack of data from remote areas such as NE Greenland. Due to these uncertainties, varied paleogeographical configurations have been used in previous modeling, ranging from open seaway to fully closed scenarios^{11,23,56,57}. Important contributions in this context include that of Hartley et al.³², who demonstrated that transient uplift pulses totaling up to 1 km offshore Scotland coincided closely with the PETM (see also refs. 30,31). These uplift pulses led to subaerial exposure for ~1 Myr, which was followed by a gradual subsidence and reburial. Similarly, Parnell-Turner et al.⁵⁸ documented pulses in Icelandic mantle plume activity leading to alternating uplift and subsidence episodes that controlled GSR height/depth later in the Eocene and Oligocene. The timing of renewed bottom current overflow over the GSR remain enigmatic³³.

Paleocene–early Eocene fragmentation of the NGS. The data presented here form an important piece in the paleogeographic puzzle by documenting Paleocene–early Eocene paleoenvironmental evolution of the NE Greenland margin (~63 to ~53 and ~48 to ~47 Ma). Our results indicate that water depth and accommodation space decreased rapidly in the western part of the NGS around the Paleocene–Eocene boundary. At least three major forced regressive episodes, with some uncertainty due to local challenges in

lateral correlation, likely related to uplift pulses, are postulated in Danian, Selandian, and Thanetian strata (Fig. 2). The interval corresponding to the Paleocene–Eocene transition and the early Eocene shows a change from offshore deposits to rapidly accumulating marine gravity flow systems, shallow marine, coarse-grained fluvial environments, and subaerial flood basalts over part of the study area (Supplementary Notes 1, 2, and 4). The offshore deposits at the base of the PETM section broadly coincide with the early PETM transgression previously reported from various parts of the world⁵⁹; however, the subsequent, strongly progradational depositional trend in the upper part of the succession was driven by regional tectonic uplift that preceded the onset of flood basalt emplacement (Fig. 2).

The flood basalt volcanism continued until at least ~53 Ma and resulted in a several km-thick sequence of subaerially extruded lavas in the present day offshore areas^{60–62}. Onshore data indicate that the intra-basaltic sediments represent thin remnants of widespread fluvial systems, paleosoils, and shallow lakes developed during erosion and ponding of fluvial incisions (Supplementary Notes 1).

The maximum extent of subaerial lavas and the immediately underlying unconformity within the context of the NGS indicate that subaerial exposure extended across the entire central and southern NE Greenland margin to the COB (Fig. 4). On the conjugate outer Norwegian Vøring and Møre margins, eastward prograding basalt deltas are suggestive of a subaerially exposed outer margin and an inundated embayment towards the east⁶³ (Fig. 1b). Collectively, these data suggest that from the Paleocene–Eocene transition to the early Eocene, a land connection from NE Greenland to the outer Norwegian margin (GNR) developed along the trend of the incipient oceanic spreading ridge. The height of the lava deltas decreases to the north, suggesting a northward shallowing of the embayment at the northernmost Vøring and Lofoten–Vesterålen margin (Fig. 1)⁶³. Structural highs delineating latest Cretaceous and early Paleogene islands or shoals straddle the Vøring and Lofoten–Vesterålen margin⁴². Consequently, NE Greenland and Europe were separated by only a narrow strait lined with islands and shoals (~50 km or less of open water). Such an environment would be sensitive to relatively minor tectonic pulses and eustatic changes, which have been estimated to be 15–30 m during the early Eocene⁶⁴ (Fig. 4). However, similarities between dinocyst assemblages between the North Sea, Western Siberia, and Arctic Ocean indicate that a marine connection persisted at least during the PETM^{53,65}.

Contemporaneously, the NGS was being restricted from the North Atlantic by transient uplift and volcanism at the GSR to the south^{30–32}. Consequently, the former seaway was fragmented into two water bodies as follows: (1) a northern marine basin connected to the western Barents Shelf, and (at least at times) the Western Siberian Basin and Arctic Ocean; and (2) a more than 1000 km-long narrow marine basin comprising the North Sea and much of the NGS that was bounded by ridges on both ends (Fig. 4). A possible shallow marine connection to the North Atlantic may have existed temporarily via the English strait⁶⁶ and via the Faroe–Shetland Basin after 54 Ma^{31,32}. The documented seaway compartmentalization refines the basin configuration used by Nisbet et al.²³, who compared the described inland sea morphology with rift lakes. The presence of the GNR adds to their model by documenting a more extreme basin restriction than previously considered, lasting at least 3–6 Myr (Fig. 4).

The post-mid Ypresian evolution of the GNR remains only loosely constrained in the absence of stratigraphic data from ~53 to ~50 Ma. Data from ODP site 913 indicate that shallow marine conditions were re-established on the nearby ocean crust at least

by ~50 Ma, denoting a transgression (Fig. 2). A transition to deep-marine conditions occurred during the early Lutetian (~47 Ma)^{36,38}, documenting a continuation of the deepening. The seismic interpretation of the contourite deposits on the outer NE Greenland margin closely overlying the lowermost Lutetian and correlated to the Kanumas 12 boreholes (Supplementary Fig. 15) tentatively suggests an onset of deep sea currents close to that time (Fig. 3d).

Implications. The PETM and early Eocene rapid warming events have been regarded as one of the most relevant ancient analogs for the current climate system. The present study contributes to understanding of the paleogeographical development of the Arctic region during this important period and suggests a revised paleogeographical configuration compared to previous works. In particular, pre-breakup uplift and NAIP emplacement led to seaway fragmentation that culminated ~56–53 Ma in the northern NGS (Fig. 4). Together with other coeval restrictions (GSR³², uplift in the pre-Fram Strait and western Barents Sea^{9,10}), the NGS–Arctic Ocean connection was characterized by a mosaic of shallow marine gateways and straits particularly during the Ypresian.

The uplifted NE Greenland margin also constituted a prominent sediment source for the offshore basins in the NGS during the Paleocene and early Eocene. The Danian–Thanetian gravity flow systems and the pre-basaltic fluvial systems prograded towards the east (see also ref. 41). However, basalts emplaced during the Ypresian formed a topographic barrier redirecting the fluvial transport towards the north and northeast (Fig. 4).

Finally, although strong and sustained north Atlantic bottom current formation probably did not take place before 34 Ma⁶⁷, seismic data from the northern North Atlantic indicate the first signs of bottom current activity in the Lutetian (~47 Ma)^{68,69}; however, the origin and significance of the current system has remained unclear. This time interval corresponds to the closure of the Arctic Ocean, a cooling climate and formation of sea ice in the Arctic (~47 Ma)^{70,71}. In our 2D seismic data sets, the Lutetian represents the first Paleogene interval where contourite drift- and moat-like features appear (Fig. 3d and Supplementary Fig. 15). Thus, although future work is needed to test the interpretation and its potential relevance for North Atlantic Deep Water formation, the data tentatively support the modeling results of Vahlenkamp et al.²¹, which indicated that a pulse of deep water formation was possible in the Nordic seas at that time, provided GSR subsidence allowed the inflow of saline waters.

Methods

Stratigraphic results. The onshore work is based on sedimentological, ichnological, and palynological data collection of selected outcrops in NE Greenland. As a survey institution, the Geological Survey of Denmark and Greenland has permits to perform data collection including sediment sampling in Greenland. The key outcrop areas include the Haredal valley (Wollaston Forland), a coastal section south of the Haredal valley, and Dronning Augustadal valley (collectively referred to as Location (loc.) 4 in Figs. 1 and 2). In addition, observations were collected from Paleogene outcrops on GSØ (Leitch Bjerg, loc. 1), Hold with Hope (Langsiden, east of Fosdalen, loc. 2), Clavering Ø (Hallebjergene, loc. 3), Sabine Ø (Germanian Havn and north side of Harefeld, loc. 5), and outliers in Wollaston Forland, including the top of the Gyldenspids Mountain. Co-ordinates for localities are provided in Supplementary Table 2. The data were collected during several field seasons: 2008–2010 (Wollaston Forland, Sabine Ø), 2010 (Hold with Hope), 2011 (GSØ), 2018 (Wollaston Forland, Sabine Ø), and 2019 (Wollaston Forland, Clavering Ø). In addition to onshore locations, cores from the Kanumas coring project sites 12 and 24 were described.

The sedimentological data collection was done at different scales due to varying outcrop quality. Ideally, the data collection included documentation of lithology, grain size and grain size trend, primary and secondary sediment structures,

bedding contacts, and paleocurrent orientation. Trace fossil content (genera, assemblage, and bioturbation intensity) were described where applicable.

Samples were processed for palynology by a methodology including treatment with hydrogen chloride, hydrogen fluoride, oxidation with nitric acid, and heavy liquid separation. At each preparation step, a slide was inspected to follow the process closely. Finally, the organic residue was sieved on a 21 µm filter (occasionally on 30 µm to concentrate palynomorphs in samples that were poor in dinocysts), then swirled and finally mounted on glass slides using a glycerin jelly medium. The dinocyst content was analyzed using a normal light microscope. Approximately 100 identifiable dinocysts per sample were counted from Kanumas site 12, the Leitch Bjerg, and the Haredal sections to perform a relative abundance analysis. Prasinophycean and freshwater algae and acritarchs in the slide were also counted in addition to the main dinocyst tally. Additional dinocyst species occurring outside the 100 counted specimens in the first slide or in other slides were recorded as present. The palynomorphs from Kanumas site 24 and the Langsiden section were not counted and only recorded as present. The palynological results are presented on the StrataBugs range charts in the Supplementary Notes 2 (Supplementary Figs. 8–14). The taxonomy used here follows that of Williams et al.⁷².

Seismic interpretation. The NE Greenland margin is covered by ~80,000 km of 2D seismic reflection data. These data include high-quality commercial data collected between 2006 and 2016, as well as a number of academic data sets and some older commercial data collected from 1991 to 1995 by the Kanumas Group (reprocessed in 2009). Seismic interpretation of the Cenozoic strata was done following well-established sequence stratigraphic concepts described by Mitchum and Vail⁷³, Mitchum et al.⁷⁴, and Sangree and Widmier⁷⁵. Seismic interpretation of the volcanic units builds on the concepts developed by Planke et al.⁷⁶, to explain the development of volcanic rifted margins.

Previous work on mapping the seismic volcanic stratigraphy of the NE Greenland margin documents a complex history of development, in particular to the south where interaction with the Jan Mayen microcontinent greatly complicates understanding the volcanic development of the initial seafloor spreading along the Central and Northeast Greenland margin^{62,77,78}. Here we simplify the interpretation to focus on the distribution of subaerially extruded lavas, which form laterally continuous top reflections underlain by either well-defined low-frequency reflections, or a transparent unit, and shallow marine units, which exhibit a hummocky ill-defined top reflection and chaotic reflectivity below.

Seismic interpretation was done using DecisionSpace Geoscience software from Landmark and included ties to the few shallow coring and ODP drill sites, providing age constraints for the Cenozoic strata (see Supplementary Fig. 15 for locations and ties). The age model was further refined by indirect age constraints obtained by: (1) correlating the volcanic vent surface observed offshore NE Greenland with the well-dated comparable vent surfaces on the Norwegian margin, which most likely reflects the same magmatic pulse^{44,45}, (2) extrapolating the age of onshore flood basalts²⁷ with flood basalts observed seismically from few kilometers offshore, and (3) correlating the stratigraphic surfaces with oceanic magnetic anomaly picks of Gaina et al.²⁵.

Paleogeographic reconstruction. No seismic interpretation was done on the conjugate Norwegian margin. The volcanic facies are based on Berndt et al.⁷⁹, and the structural features and age inferences are based on publicly available information from the Norwegian Petroleum Directorates web site (<https://www.npd.no>). To infer the likely paleogeography near the Paleocene–Eocene boundary, the essential features mapped on the East Greenland margin were rotated to a fixed European plate at 56 Ma using the poles of rotation in Gaina et al.²⁵. Areas inferred to have been subaerial based on the above stratigraphic and mapping considerations were then outlined.

Data availability

The Kanumas cores and palynological slides are stored by the Geological Survey of Denmark and Greenland (www.geus.dk). Released seismic data are available via www.greenpetrodata.gl or through the GEUS data archive (data@geus.dk). Data collected in 2014–2016 are available from the data vendor TGS (www.tgs.com/) but restrictions apply to their availability until 2023 when their confidentiality period ends. However, 2014–2016 data may be made available for academic purposes through direct negotiation with TGS.

Received: 5 December 2020; Accepted: 30 July 2021;

Published online: 23 August 2021

References

1. Storey, M., Duncan, R. A. & Tegner, C. Timing and duration of volcanism in the North Atlantic Igneous Province: implications for geodynamics and links to the Iceland hotspot. *Chem. Geol.* **241**, 264–281 (2007).
2. Horni, J. Á. et al. Regional distribution of volcanism within the North Atlantic Igneous Province in The NE Atlantic Region: a reappraisal of crustal structure, tectonostratigraphy and magmatic evolution. *Geol. Soc. Spec. Publ.* **447**, 105–125, <https://doi.org/10.1144/sp447.18> (2017).
3. O'Regan, M. et al. Mid-Cenozoic tectonic and paleoenvironmental setting of the central Arctic Ocean. *Paleoceanography* **23**, PA1520 (2008).
4. Døssing, A., Hopper, J. R., Olesen, A. V., Rasmussen, T. M. & Halpenny, J. New aero-gravity results from the Arctic: linking the latest Cretaceous-early Cenozoic plate kinematics of the North Atlantic and Arctic Ocean. *Geochem. Geophys.* **14**, 4044–4065 (2013).
5. Jokat, W., Ickrath, M. & O'Connor, J. Seismic transect across the Lomonosov and Mendeleev Ridges: constraints on the geological evolution of the Amerasia Basin, Arctic Ocean. *Geophys. Res. Lett.* **GL057275**, <https://doi.org/10.1002/grl.50975> (2013).
6. Døssing, A., Hansen, T. M., Olesen, A. V., Hopper, J. R. & Funck, T. Gravity inversion predicts the nature of the Amundsen Basin and its continental borderlands near Greenland. *Earth Planet. Sci. Lett.* **408**, 132–145 (2014).
7. Gaina, C., Nikishin, A. M. & Petrov, E. I. Ultraslow spreading, ridge relocation and compressional events in the East Arctic region: a link to the Eureka orogeny? *Arktos* **1**, 16 (2015).
8. Piepjohn, K., von Gosen, W. & Tessensohn, F. The Eureka deformation in the Arctic: an outline. *J. Geol. Soc. Lond.* **173**, 1007–1024 (2016).
9. Lasabuda, A., Laberg, J. S., Knutsen, S.-M. & Safronova, P. Cenozoic tectonostratigraphy and pre-glacial erosion: a mass-balance study of the northwestern Barents Sea margin, Norwegian Arctic. *J. Geodyn.* **119**, 149–166 (2018a).
10. Lasabuda, A., Laberg, J. S., Knutsen, S.-M. & Høgseth, G. Early to middle Cenozoic paleoenvironment and erosion estimates of the southwestern Barents Sea: insights from a regional mass-balance approach. *Mar. Pet. Geol.* **96**, 501–521 (2018b).
11. Brinkhuis, H. et al. Episodic fresh surface waters in the Eocene Arctic Ocean. *Nature* **441**, 606–609 (2006).
12. Akhmetiev, M. A. et al. The Paleogene history of the Western Siberian seaway — a connection of the Peri-Tethys to the Arctic Ocean. *Austrian J. Earth Sci.* **105**, 50–67 (2012).
13. Nikishin, A. M. et al. Geological structure and history of the Arctic Ocean based on new geophysical data: Implications for paleoenvironment and paleoclimate. Part 2. Mesozoic to Cenozoic geological evolution. *Earth Sci. Rev.* **103034**, <https://doi.org/10.1016/j.earscirev.2019.103034> (2019).
14. Somme, T. O., Doré, A. G., Lundin, E. R. & Tørudbakken, B. O. Triassic–Paleogene paleogeography of the Arctic: implications for sediment routing and basin fill. *Am. Assoc. Pet. Geol. Bull.* **102**, 2481–2517 (2018).
15. Blakey, R. Paleotectonic and paleogeographic history of the Arctic region. *Atl. Geol.* **57**, 007–039 (2021).
16. Aubry, M.-P., Ouda, K., Dupuis, C., Berggren, W. A. & Van Couvering, J. A., The Members of the Working Group on the Paleocene/Eocene Boundary. The global standard stratotype-section and point (GSSP) for the base of the Eocene series in the Dababiya section (Egypt). *Episodes* **30**, 271–286 (2007).
17. Westerhold, T. et al. An astronomically dated record of Earth's climate and its predictability over the last 66 million years. *Science* **369**, 1383–1387 (2020).
18. Bice, K. L. & Marotzke, J. Could changing ocean circulation have destabilized methane hydrate at the Palaeocene/Eocene boundary? *Paleoceanography* **17**, 8-1–8-12 (2002).
19. Roberts, C. D., LeGrande, A. N. & Tripati, A. K. Climate sensitivity to Arctic seaway restriction during the early Paleogene. *Earth Planet. Sci. Lett.* **286**, 576–585 (2009).
20. Stårz, M., Jokat, W., Knorr, G. & Lohmann, G. Threshold in North Atlantic–Arctic Ocean circulation controlled by the subsidence of the Greenland–Scotland Ridge. *Nat. Commun.* **8**, 15681 (2017).
21. Vahlenkamp, M. et al. Ocean and climate response to North Atlantic seaway changes at the onset of long-term Eocene cooling. *Earth Planet. Sci. Lett.* **498**, 185–195 (2018).
22. Hutchinson, D. K. et al. Arctic closure as a trigger for Atlantic overturning at the Eocene–Oligocene Transition. *Nat. Commun.* **10**, 3797 (2019).
23. Nisbet, E. G. et al. Kick-starting ancient warming. *Nat. Geosci.* **2**, 156–159 (2009).
24. Surlyk, F. The Jurassic of East Greenland: a sedimentary record of thermal subsidence, onset and culmination of rifting. *Geol. Surv. Den. Greenl. Bull.* **1**, 659–722 (2003).
25. Gaina, C., Nasuti, A., Kimbell, G. S. & Blischke, A. Break-up and seafloor spreading domains in the NE Atlantic. *Geol. Soc. Spec. Publ.* **447**, 393–417 (2017).
26. Gernigon, L. et al. Crustal fragmentation, magmatism, and the diachronous opening of the Norwegian–Greenland Sea. *Earth Sci. Rev.* **206**, <https://doi.org/10.1016/j.earscirev.2019.04.011> (2020).
27. Larsen, L. M., Pedersen, A. K., Tegner, C. & Duncan, R. A. Eocene to Miocene igneous activity in NE Greenland: northward younging of magmatism along the East Greenland margin. *J. Geol. Soc. Lond.* **171**, 539–553 (2014).
28. Steinberger, B., Bredow, E., Lebedev, S., Schaeffer, A. & Torsvik, T. H. Widespread volcanism in the Greenland–North Atlantic region explained by the Iceland plume. *Nat. Geosci.* **12**, 61–68 (2019).

29. Bott, M. H. P., Saxov, S., Talwani, M. & Thiede, J. *Structure and Development of the Greenland-Scotland Ridge. Nato Conference Series (IV Marine Science) Vol. 8* (Springer, 1983).
30. MacLennan, J. & Jones, S. M. Regional uplift, gas hydrate dissociation and the origins of the Paleocene–Eocene Thermal Maximum. *Earth Planet. Sci. Lett.* **245**, 65–80 (2006).
31. Shaw Champion, M. E., White, N. J., Jones, S. M. & Lovell, J. P. B. Quantifying transient mantle convective uplift: an example from the Faroe-Shetland basin. *Tectonics* **27**, TC1002 (2008).
32. Hartley, R. A., Roberts, G. G., White, N. & Richardson, C. Transient convective uplift of an ancient buried landscape. *Nat. Geosci.* **4**, 562–565 (2011).
33. Uenzelmann-Neben, G. & Gruetznern, J. Chronology of Greenland Scotland Ridge overflow: what do we really know? *Marine Geol.* **406**, 109–118 (2018).
34. Jolley, D. W. & Whitham, A. G. A stratigraphical and palaeoenvironmental analysis of the sub-basaltic Palaeogene sediments of East Greenland. *Pet. Geosci.* **10**, 53–60 (2004).
35. Nøhr-Hansen, H., Nielsen, L. H., Sheldon, E., Hovikoski, J. & Alsen, P. Paleogene deposits in North-East Greenland. *Geol. Surv. Den. Greenl. Bull.* **23**, 61–64 (2011).
36. Hull, D. L., Osterman, I. E. & Thiede, J. Bio-stratigraphic synthesis of Leg 151, North Atlantic–Arctic gateways. *Proc. Ocean Drill. Program Sci. Results* **151**, 627–644 (1996).
37. Brekke, H., Sjulstad, H. I., Magnus, C. & Williams, R. W. Sedimentary environments offshore Norway: an overview. *Norwegian Pet. Soc. Special Publ.* **10**, 7–37 (2001).
38. Eldrett, J. S., Harding, I. C., Firth, J. V. & Roberts, A. P. Magnetostratigraphic calibration of Eocene–Oligocene dinoflagellate cyst biostratigraphy from the Norwegian–Greenland Sea. *Mar. Geol.* **204**, 91–127 (2004).
39. Petersen, T. G. Seismic stratigraphy of the post-breakup succession offshore Northeast Greenland: links to margin uplift. *Mar. Pet. Geol.* **103**, 422–437 (2019).
40. Polteau, S. et al. The pre-breakup stratigraphy and petroleum system of the Southern Jan Mayen Ridge revealed by seafloor sampling. *Tectonophysics* **760**, 152–164 (2019).
41. Polteau, S. et al. Upper Cretaceous–Paleogene stratigraphy and development of the Mimir High Vøring Transform Margin, Norwegian Sea. *Mar. Pet. Geol.* **122**, 104717 (2020).
42. Zastrozhnov, D. et al. Regional structure and polyphased Cretaceous–Paleocene rift and basin development of the mid-Norwegian volcanic passive margin. *Mar. Pet. Geol.* **115**, 104269 (2020).
43. Petersen, T. G. New sequence stratigraphic framework on a ‘passive’ margin: implications for the post-break-up depositional environment and onset of glaciomarine conditions in NE Greenland. *J. Geol. Soc. Lond.* **178**, <https://doi.org/10.1144/jgs2020-128> (2021).
44. Reynolds, P. et al. Hydrothermal vent complexes offshore Northeast Greenland: A potential role in driving the PETM. *Earth Planet. Sci. Lett.* **467**, 72–78 (2017).
45. Svensen, H. et al. Release of methane from a volcanic basin as a mechanism for initial Eocene global warming. *Nature* **429**, 542–545 (2004).
46. Frieling, J. et al. Thermogenic methane release as a cause for the long duration of the PETM. *Proc. Natl Acad. Sci. USA* **113**, 12059–12064 (2016).
47. van der Burgh, J., Collinson, M. E., van Konijnenburg-van Cittert, J. H., Barke, J. & Brinkhuis, H. The freshwater fern Azolla (Azollaceae) from Eocene Arctic and Nordic Sea sediments: New species and their stratigraphic distribution. *Rev. Palaeobot. Palynol.* **194**, 50–68 (2013).
48. Jess, S. & Peace, A. Sediment supply on the West Greenland passive margin: redirection of a large pre-glacial drainage system. *J. Geol. Soc.* **177**, 1149–1160 (2020).
49. Dam, G. & Sønderholm, M. Tectonostratigraphic evolution, palaeogeography and main petroleum plays of the Nuussuaq Basin: an outcrop analogue for the Cretaceous–Palaeogene rift basins offshore West Greenland. *Mar. Pet. Geol.* **129**, 105047 (2021).
50. Smelror, M., Petrov, O. V., Larssen, G. B. & Werner, S. *Atlas: Geological History of the Barents Sea* (Geological Survey of Norway, 2009).
51. Straume, E. O., Gaina, C., Medvedev, S. & Nisancioglu, K. H. Global Cenozoic Paleobathymetry with a focus on the Northern Hemisphere Oceanic Gateways. *Gondwana Res.* <https://doi.org/10.1016/j.gr.2020.05.011> (2020).
52. Japsen, P., Green, P. F. & Chalmers, J. A. Thermo-tectonic development of the Wandel Sea Basin, North Greenland. *Geol. Surv. Den. Greenl. Bull.* **45**, <https://doi.org/10.34194/geusb.v45.5298> (2021).
53. Iakovleva, A. I., Brinkhuis, H. & Cavagnetto, C. Late Palaeocene–early Eocene dinoflagellate cysts from the Turgay Strait, Kazakhstan; correlations across ancient seaways. *Palaeogeogr. Palaeoclimatol. Palaeoecol.* **172**, 243–268 (2001).
54. Iakovleva, A. I. & Kulkova, I. A. Paleocene–Eocene dinoflagellate zonation of Western Siberia. *Rev. Palaeobot. Palynol.* **123**, 185–197 (2003).
55. Akhmetiev, M. A. et al. Comparative analysis of marine Paleogene sections and biota from West Siberia and the Arctic Region. *Stratigr. Geol. Correl.* **18**, 78–103 (2010).
56. Kender, S. et al. Marine and terrestrial environmental changes in NW Europe preceding carbon release at the Paleocene–Eocene transition. *Earth Planet. Sci. Lett.* **353–354**, 108–120 (2012).
57. Alexander, K., Meissner, J. K. & Bralower, T. J. Sudden spreading of corrosive bottom water during the Palaeocene–Eocene Thermal Maximum. *Nat. Geosci.* **8**, 458–461 (2015).
58. Parnell-Turner, R. et al. A continuous 55-million-year record of transient mantle plume activity beneath Iceland. *Nat. Geosci.* **7**, 914–919 (2014).
59. Sluijs, A. et al. Eustatic variations during the Paleocene–Eocene greenhouse world. *Paleoceanography* **23**, PA4216 (2008).
60. Hopper, J. R. et al. Structure of the SE Greenland margin from seismic reflection and refraction data: implications for nascent spreading center subsidence and asymmetric crustal accretion during North Atlantic opening. *J. Geophys. Res.* **108**, <https://doi.org/10.1029/2002JB001996> (2003).
61. Voss, M. & Jokat, W. Continent–ocean transition and voluminous magmatic underplating derived from P-wave velocity modelling of the East Greenland continental margin. *Geophys. J. Int.* **170**, 580–604 (2007).
62. Franke, D. et al. Polyphase magmatism during the formation of the northern East Greenland continental margin. *Tectonics*, **38**, <https://doi.org/10.1029/2019TC005552> (2019).
63. Abdelmalak, M. M. et al. The development of volcanic sequences at rifted margins: New insights from the structure and morphology of the Vøring Escarpment, mid-Norwegian Margin. *J. Geophys. Res. Solid Earth* **121**, 5212–5236 (2016).
64. Miller, K. et al. Cenozoic sea-level and cryospheric evolution from deep-sea geochemical and continental margin records. *Sci. Adv.* <https://doi.org/10.1126/sciadv.aaz1346> (2020).
65. Sluijs, A. et al. Arctic late Paleocene–early Eocene paleoenvironments with special emphasis on the Paleocene–Eocene thermal maximum (Lomonosov Ridge, Integrated Ocean Drilling Program Expedition 302). *Paleoceanography* **23**, PA1511 (2008).
66. Zacke, A. et al. Surface-water freshening and high latitude river discharge in the Eocene of the North Sea. *J. Geol. Soc. London* **166**, 969–980 (2009).
67. Ferreira, D. et al. Atlantic–Pacific asymmetry in deep-water formation. *Annu. Rev. Earth Planet. Sci.* **46**, 327–352 (2018).
68. Boyle, P. R. et al. Cenozoic North Atlantic deep circulation history recorded in contourite drifts, offshore Newfoundland, Canada. *Mar. Geol.* **385**, 185–203 (2017).
69. Hohbein, M. W., Sexton, P. F. & Cartwright, J. A. Onset of North Atlantic Deep Water production coincident with inception of the Cenozoic global cooling trend. *Geology* **40**, 255–258 (2012).
70. Stickley, C. E. et al. Evidence for middle Eocene Arctic Sea ice from diatoms and ice-rafted debris. *Nature* **460**, 376–379 (2009).
71. Tripathi, A. & Darby, D. Evidence for ephemeral middle eocene to early oligocene greenland glacial ice and pan-arctic sea ice. *Nat. Commun.* **9**, 1038 (2018).
72. Williams, G. L., Fensome, R. A. & MacRae, R. A. DINOFLAJ3. American Association of Stratigraphic Palynologists, Data Series no. 2. <http://dinoflaj.smu.ca/dinoflaj3> (2017).
73. Mitchum, R. M. Jr. & Vail, P. R. In *Seismic Stratigraphy—Application to Hydrocarbon Exploration* (ed. Payton, C. E.) 26, 135–143 (AAPG Memoir, 1977).
74. Mitchum, R. M. Jr., Vail, P. R. & Sangree, J. In *Seismic Stratigraphy—Application to Hydrocarbon Exploration* (ed. Payton, C. E.) 26, 117–133 (AAPG Memoir, 1977).
75. Sangree, J. B. & Widmier, J. M. In *Seismic Stratigraphy—Application to Hydrocarbon Exploration* (ed. Payton, C. E.) 26, 165–184 (AAPG Memoir, 1977).
76. Planke, S., Symonds, P. A., Alvestad, E. & Skogseid, J. Seismic volcanostratigraphy of large-volume basaltic extrusive complexes on rifted margins. *J. Geophys. Res.* **105**, 19335–19351 (2000).
77. Geissler, W. H. et al. In *The NE Atlantic Region: A Reappraisal of Crustal Structure, Tectonostratigraphy and Magmatic Evolution* (eds. G. Pinvidic et al.), 149–170 (Geological Society of London, 2017).
78. Blischke, A. et al. The Jan Mayen microcontinent: an update of its architecture, structural development and role during the transition from the Ægir Ridge to the mid-oceanic Kolbeinsey Ridge. *Geol. Soc. Spec. Publ.* **447**, 299–337 (2016).
79. Berndt, C., Planke, S., Alvestad, E., Tsikalas, F. & Rasmussen, T. Seismic volcanostratigraphy of the Norwegian Margin: constraints on tectonomagmatic break-up processes. *J. Geol. Soc. Lond.* **158**, 413–426 (2001).
80. Hopper, J. R. et al. (eds). *Tectonostratigraphic Atlas of the North-East Atlantic Region 338* (Geological Survey of Denmark and Greenland (GEUS), 2014).
81. Pedersen, M., Weng, W. L., Keulen, N. & Kokfelt, T. F. A new seamless digital 1:500 000 scale geological map of Greenland. *Geol. Surv. Den. Greenl. Bull.* **28**, 65–68 (2013).

82. Parsons, A. J. et al. Structural evolution and basin architecture of the Traill Ø region, NE Greenland: a record of polyphase rifting of the East Greenland continental margin. *Geosphere* **13**, 733–770 (2017).
83. Watt, W. S. Stratigraphy and correlation of the Tertiary plateau basalts in North-East Greenland. *Rapport Grønlands Geologiske Undersøgelse* **162**, 185–194 (1994).
84. Onodera, J., Takahashi, K. & Jordan, R. W. Eocene silicoflagellate and ebridian paleoceanography in the central Arctic Ocean. *Paleoceanography* **23**, PA1S15 (2008).

Acknowledgements

GEUS and the ministry of mineral resources (Government of Greenland) funded data collection in Wollaston Forland and Clavering Ø areas. Other work was funded by GEUS. Insightful comments by Matt O'Regan, Henk Brinkhuis, and Stéphane Polteau are greatly appreciated. We thank Jette Halskov for skillful drafting of the figures.

Author contributions

J.H., M.B.W.F., H.N.-H. and J.R.H. wrote the paper with contributions from others. Sedimentological data collection and interpretation was done by J.H., S.A., M. Barham, L.H.N. and M. Bjerager with contributions from J.B.-K., S.L., A.U., P.A., E.S. and P.R.S. Palynological data were collected and interpreted by H.N.-H. Seismic data were interpreted by M.B.W.F. and J.R.H. J.R.H. made the G-plate reconstruction.

Competing interests

The authors declare no competing interests.

Additional information

Supplementary information The online version contains supplementary material available at <https://doi.org/10.1038/s43247-021-00249-w>.

Correspondence and requests for materials should be addressed to J.H.

Peer review information *Communications Earth & Environment* thanks Matt O'Regan, Henk Brinkhuis, and the other, anonymous, reviewer(s) for their contribution to the peer review of this work. Primary Handling Editors: João Duarte and Joe Aslin.

Reprints and permission information is available at <http://www.nature.com/reprints>

Publisher's note Springer Nature remains neutral with regard to jurisdictional claims in published maps and institutional affiliations.



Open Access This article is licensed under a Creative Commons Attribution 4.0 International License, which permits use, sharing, adaptation, distribution and reproduction in any medium or format, as long as you give appropriate credit to the original author(s) and the source, provide a link to the Creative Commons license, and indicate if changes were made. The images or other third party material in this article are included in the article's Creative Commons license, unless indicated otherwise in a credit line to the material. If material is not included in the article's Creative Commons license and your intended use is not permitted by statutory regulation or exceeds the permitted use, you will need to obtain permission directly from the copyright holder. To view a copy of this license, visit <http://creativecommons.org/licenses/by/4.0/>.

© The Author(s) 2021